Synthesis and Properties of Azidonitrophenyl Pyrophosphate, a Photoaffinity Probe of the Nucleotide Binding Sites of Mitochondrial F_1-ATPase†

Laurent Michel, Jérôme Garin,* Jean-Paul Issartel, and Pierre V. Vignais
Laboratoire de Biochimie, Département de Recherche Fondamentale, Centre d'Etudes Nucléaires, 85X, 38041 Grenoble Cedex, France

Received May 2, 1989; Revised Manuscript Received July 28, 1989

ABSTRACT: 4-Azido-2-nitrophenyl pyrophosphate (azido-PP_i) labeled with ^{32}P in the α position was prepared and used to photolabel beef heart mitochondrial F_1. Azido-PP_i was hydrolyzed by yeast inorganic pyrophosphatase, but not by mitochondrial F_1-ATPase. Incubation of F_1 with [α-^{32}P]azido-PP_i in the dark under conditions of saturation resulted in the binding of the photoprobe to three sites, two of which exhibited a high affinity (K_d = 2 μM), the third one having a lower affinity (K_d = 300 μM). Mg^{2+} was required for binding. As with PP_i [Issartel et al. (1987) *J. Biol. Chem. 262*, 13538-13544], the binding of 3 mol of azido-PP_i/mol of F_1 resulted in the release of one tightly bound nucleotide. ADP, AMP-PNP, and PP_i competed with azido-PP_i for binding to F_1, but P_i and the phosphate analogue azidonitrophenyl phosphate did not. The binding of [^{32}P]P_i to F_1 was enhanced at low concentrations of azido-PP_i, as it was in the presence of low concentrations of PP_i. Sulfite, which is thought to bind to an anion-binding site on F_1, inhibited competitively the binding of both ADP and azido-PP_i, suggesting that the postulated anion-binding site of F_1 is related to the exchangeable nucleotide-binding sites. Upon photoirradiation of F_1 in the presence of [α-^{32}P]azido-PP_i, the photoprobe became covalently bound with concomitant inactivation of F_1. The plots relating the inactivation of F_1 to the covalent binding of the probe were rectilinear up to 50% inactivation. Extrapolation of the rectilinear portion of the curve to the abscissa indicated that 100% inactivation was attained upon binding of 1.1 mol of azido-PP_i/mol of F_1. Both the α and β subunits of F_1 were photolabeled with a predominance of photolabeling on the β subunit. The presence of PP_i and ADP in the incubation medium efficiently protected F_1 against photolabeling.

The F_1[1] sector of mitochondrial ATPase is a multimeric complex composed of five types of subunits; α and β are the major functional subunits and bear all the ligand binding sites [for review cf. Vignais and Lunardi (1985)]. During the course of ATP hydrolysis, three of the six nucleotide-binding sites of F_1 rapidly exchange their bound nucleotides with ATP. On the other hand, there is only one titrable high-affinity binding site for P_i per F_1, and the fact that P_i binding is affected by nucleotides suggests that the P_i binding site is part of the catalytic site. Furthermore, the behavior of F_1 is also affected by certain anions, including sulfite, though it is not known whether this reflects a conformational change or an interaction with specific sites.

In a previous study bearing on the substrate binding sites of mitochondrial F_1, it was found that PP_i mimicked ADP more closely than it did P_i, probably due to its analogy with the phosphate chain of ADP (Issartel et al., 1987). The photoprobes used so far for mapping studies of the substrate binding sites of F_1 were nucleotide analogues modified in the purine ring or the ribose moiety [for review cf. Vignais and Lunardi (1985)] and a P_i analogue (Garin et al., 1989). In this paper, we report the synthesis and the binding properties of a photoactivable derivative of PP_i, the azidonitrophenyl pyrophosphate (azido-PP_i). The perfect mimicry of PP_i by azido-PP_i makes azido-PP_i a suitable tool for mapping the portion of the nucleotide-binding site of F_1 that interacts with the phosphate chain of ADP or ATP. The combined use of azidonitrophenyl phosphate (ANPP) and azido-PP_i should prove to be particularly useful in this respect. Furthermore, as azido-PP_i is a substrate for pyrophosphatases, it should provide the means to explore the catalytic sites of these enzymes.

Materials and Methods

Chemicals. 4-Amino-2-nitrophenol was from Fluka, 1,1′-carbonyldiimidazole and silica gel 60F254 aluminum plates were from Merck, and acetonitrile was from BDH. Yeast inorganic pyrophosphatase (EC 3.6.1.1, pyrophosphate phosphohydrolase, M_r = 68 000) was obtained as an ammonium sulfate suspension from Boehringer. Luciferin–luciferase mixture was from LKB. [^{32}P]Phosphoric acid and sodium [^{32}P]pyrophosphate were purchased from New England Nuclear. The latter was diluted with unlabeled pyrophosphate to a specific radioactivity ranging between 200 and 400 dpm/pmol. [8-^3H]ADP was from Amersham. Sephadex G-50 fine grade was from Pharmacia. All reagents used were of the purest grade commercially available; those used in the synthesis of [α-^{32}P]azido-PP_i were redistilled.

Preparation of Mitochondrial F_1. F_1 was isolated from beef heart mitochondria according to the method of Knowles and Penefsky (1972) as modified by Klein et al. (1982). It was stored at 4 °C as a suspension in 50 mM Tris-HCl, 250 mM sucrose, 2 mM EDTA, 4 mM ATP, and 2.1 M $(NH_4)_2SO_4$, final pH 8.0. Before use, an aliquot sample was centrifuged, and the pellet was dissolved in 250 mM sucrose and 50 mM Tris–acetate at pH 7.5 and desalted by centrifugation–filtration in a 1-mL syringe filled with Sephadex G-50 fine grade equilibrated in the same buffer (Penefsky, 1977). Finally, the filtrate containing F_1 was passed through a second Sephadex

† This work was funded in part by grants from the Centre National de la Recherche Scientifique (UA 1130) and the Université Joseph Fourier, Faculté de Médecine de Grenoble.

[1] Abbreviations: F_1, catalytic sector of H^+-dependent mitochondrial ATPase; azido-PP_i, 4-azido-2-nitrophenyl pyrophosphate; ANPP, 4-azido-2-nitrophenyl phosphate; AMP-PNP, 5′-adenylyl imidodiphosphate; HEPES, 4-(2-hydroxyethyl)-1-piperazineethanesulfonic acid.

0006-2960/89/0428-10022$01.50/0

G-50 column equilibrated in the incubation medium to be used. F_1 prepared, stored, and desalted as described above contains three endogenous nucleotides consisting of two ADP and one ATP (Issartel et al., 1987). Nucleotide-depleted F_1 was prepared as described by Garrett and Penefsky (1975).

Binding Measurements. F_1 freed of loosely bound nucleotides was incubated in the dark at a final concentration of about 1 μM with increasing concentrations of labeled ligands, namely [α-^{32}P]azido-PP_i, [^{32}P]P_i, [^{32}P]PP_i, or [^{3}H]ADP, in 0.1 mL of a sucrose–saline medium consisting of 150 mM sucrose, 15 mM Tris-HCl, 50 mM NaCl, 3 mM $MgCl_2$, and 10% glycerol (w/v), final pH 7.5 (medium A). After a 30-min incubation at 30 °C, the samples were subjected to a centrifugation–filtration step through Sephadex G-50. Molar concentrations of purified F_1 were calculated on the basis of a molecular mass of 371 kDa (Walker et al., 1985). The protein concentration was determined by the method of Bradford (1976) with bovine serum albumin as standard.

Tightly bound nucleotides were released after heat denaturation of F_1 as described by Issartel et al. (1986) and assayed by a luminescence test using a luciferin–luciferase mixture (Lundin et al., 1976).

Assay of F_1-ATPase Activity. ATPase activity of F_1 was measured at 30 °C. The ATP-regenerating medium, in a final volume of 0.5 mL, contained 40 mM Tris-HCl, 10 mM ATP, 5 mM $MgCl_2$, 10 μg of pyruvate kinase, and 2 mM phosphoenolpyruvate, final pH 8.0. The released P_i was determined by the method of Fiske and Subbarow (1925).

Radioactivity Determination. Aqueous radioactive solutions (1.0-mL fractions) were dispersed in 10 mL of a ready-made scintillation fluid (Beckman). Radioactivity was measured by scintillation counting.

Substrate Hydrolysis by Mitochondrial F_1-ATPase and Yeast Inorganic Pyrophosphatase. The incubation medium (0.1 mL) consisted of 25 mM Tris-HCl and 3 mM $MgCl_2$, final pH 8.0, for the assay of F_1-ATPase, and 50 mM HEPES, 10 mM $MgCl_2$, and 10 mM KCl, final pH 7.0, for the assay of pyrophosphatase. The radiolabeled ligands were used at the final concentration of 0.1 mM. The final concentrations of F_1-ATPase and pyrophosphatase were 1.4 μM. Incubation was for 3 h at 30 °C. Samples of the reaction medium were chromatographed on silica gel plates by using the procedure of Bronnikov and Zakharov (1983), recently modified for a better separation of ATP and P_i (Issartel et al., 1987). Briefly, the solvent phase used to develop the chromatography was dioxane, 2-propanol, 20% NH_4OH, and H_2O (40/20/50/30) containing 9 mM EDTA. The labeled products were visualized by autoradiography.

Photolabeling Experiments. F_1-ATPase was desalted by the two-step procedure described above, incubated in medium A at a final concentration of 2.7 μM, and incubated for 30 min at 30 °C in the dark with [^{32}P]azido-PP_i. It was then subjected to four successive photoirradiations of 30 s with a xenon XB 100 lamp (1000 W) equipped with a parabolic reflector and placed 30 cm from the preparations. Protection against deleterious short-wavelength UV radiations was achieved by placing a glass plate between the light source and the samples.

The determination of the covalently bound photoprobe was carried out as follows. The photoirradiated F_1-ATPase was incubated with 4 mM PP_i for 15 min at 30 °C to chase the noncovalently bound probe and finally recovered in the excluded fraction after elution–centrifugation through a 1-mL Sephadex G-50 column equilibrated in medium A. An aliquot fraction was then assayed for ATPase activity, while the remaining was denatured either by heat (5 min at 95 °C) or acid treatment (10 min with TCA 15% at 0 °C). The denatured enzyme was then sedimented by centrifugation for 15 min at 15000*g*. The pellet was resuspended in 100% formic acid and assayed for bound radioactivity and protein content.

Several unlabeled ligands were checked for their protective effect against photolabeling. They were included with the photoprobe in the incubation medium prior to photoirradiation. The photolabeled enzyme was recovered after centrifugation–filtration through a column of Sephadex G-50 equilibrated with 10 mM Tris-HCl, pH 7.5. Labeling of subunits was explored by TDAB–polyacrylamide gel electrophoresis (Penin et al., 1984) followed by autoradiography.

Synthesis of 4-Azido-2-nitrophenyl [α-^{32}P]Pyrophosphate ([α-^{32}P]Azido-PP_i). The first step was the synthesis of 4-azido-2-nitrophenyl [^{32}P]phosphate ([^{32}P]ANPP) from 4-azido-2-nitrophenol and [^{32}P]P_i (10 mCi) by an improved version (Garin et al., 1989) of the original method developed by Lauquin et al. (1980). The purity of [^{32}P]ANPP was checked by thin-layer chromatography on silica gel plates using the same phase as that previously described. A single radioactive and UV-absorbing spot was revealed, with a R_f of 0.90. The yield of synthesis of [^{32}P]ANPP was about 40% with respect to the added [^{32}P]P_i.

The second step consisted of the phosphorylation of [^{32}P]-ANPP into [α-^{32}P]azido-PP_i. The method of Hoard and Ott (1965) was used with 10 μmol of [^{32}P]ANPP activated by 100 μmol of 1,1′-carbonyldiimidazole and 50 μmol of the tri-*n*-butylammonium salt of P_i. To purify the [α-^{32}P]azido-PP_i, the reaction mixture was dried, redissolved in 1 mL of water, and then subjected to reverse-phase HPLC chromatography using a C_{18} μBondapak preparative column (Waters) and phosphate-free solvents, namely TFA, water, and acetonitrile. As illustrated in Figure 1A, [^{32}P]P_i and [^{32}P]PP_i were eluted in fractions 7 and 8, whereas [α-^{32}P]azido-PP_i was recovered in fractions 12 and 13 and unreacted [^{32}P]ANPP in fractions 15–17. The purity of [α-^{32}P]azido-PP_i was checked by thin-layer chromatography on silica gel plates using the same phase as that previously described. A major radioactive and UV-absorbing spot was revealed, with a R_f of 0.56. At this stage, the product was 90–98% pure depending on preparations. Accordingly, purification was pursued. The pooled fractions 12 and 13 were evaporated to dryness. The residue was redissolved in 2 mL of water and applied to a DE 52 anion-exchange column (Whatman) equilibrated with saturated $NaHCO_3$. Elution was carried out with a linear gradient of 2 L of 0–0.5 M triethylammonium bicarbonate, pH 7.5, and the collected fractions (10 mL) were assayed for radioactivity. Residual [^{32}P]ANPP was eluted first, followed by [α-^{32}P]-azido-PP_i (not shown). The fractions containing [α-^{32}P]azido-PP_i were evaporated to dryness, and the residue was dissolved in 1 mL of water. The purity of [α-^{32}P]azido-PP_i was assessed by thin-layer chromatography (Figure 1B). On the basis of UV absorbance and radioactivity measurement, the yield of [α-^{32}P]azido-PP_i was estimated to about 30% with respect to initial [^{32}P]ANPP. Its specific activity ranged between 500 and 1000 dpm/pmol. UV spectra in 0.1 N HCl showed maxima at 247 and 335 nm with ϵ_{247} = 20 500 M^{-1} cm^{-1} and a ϵ_{247} to ϵ_{335} ratio of 11.4 (Figure 2A).

Results

Physical Characterization of Azido-PP_i. The effect of high-intensity light flashes on the spectrum of azido-PP_i is illustrated in Figure 2A. The decrease in absorbance at 247 nm was accompanied by a progressive increase of absorbance at 300 nm. The absorbance of the secondary peak at 340 nm

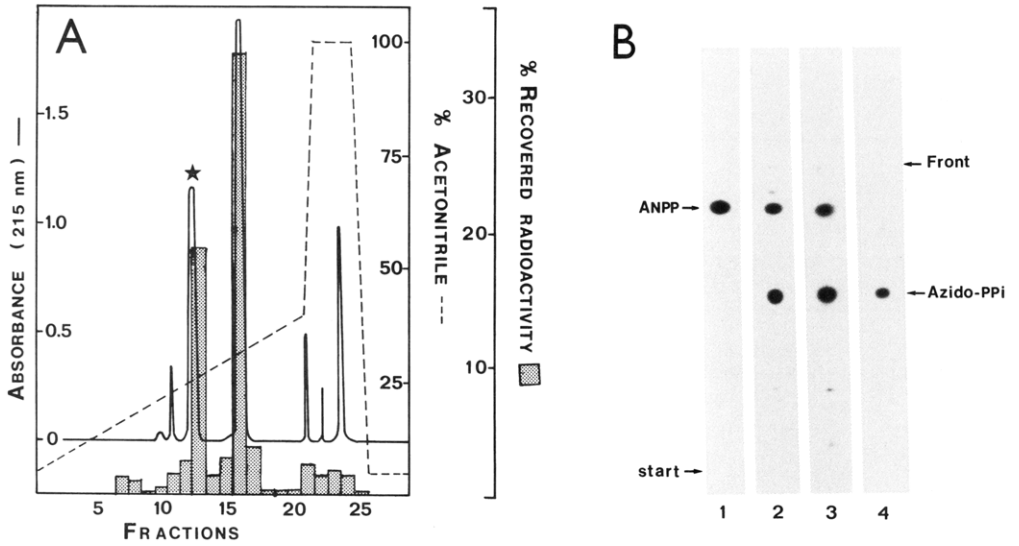

FIGURE 1: (A) Purification of [α-^{32}P]azido-PP$_i$ by HPLC. The column (Waters, C_{18} preparative) was equilibrated in 95% 0.1% TFA and 5% of a mixture of 0.1% TFA and 99.9% acetonitrile. The [α-^{32}P]azido-PP$_i$ solution (about 1 mL) was injected into the column in 200-μL fractions, and a linear gradient of acetonitrile up 99.9% in 0.1% TFA was applied at a flow rate of 2 mL min^{-1}. Fractions were collected at 1-min intervals. (B) Analysis of products of phosphorylation of ANPP by chromatography on silica gel plates followed by autoradiography. (Lane 1) Pure [^{32}P]ANPP; (lane 2) products of phosphorylation of [^{32}P]ANPP; (lane 3) partially purified [α-^{32}P]azido-PP$_i$ obtained after HPLC; (lane 4) pure [α-^{32}P]azido-PP$_i$ obtained after DE 52 chromatography.

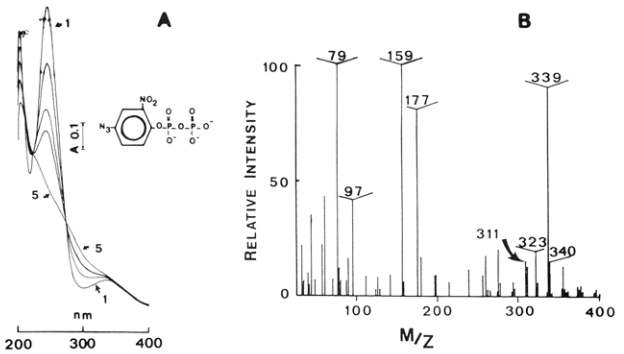

FIGURE 2: (A) Absorbance spectrum and photoreactivity of azido-PP$_i$. A solution of azido-PP$_i$ (76 μM in 0.1 N HCl) in a quartz cuvette of 1-cm pathway was submitted to successive flashes of light delivered by a VL 6L lamp placed 5 cm from the cuvette. (Trace 1) Control; (trace 2) 10-s flash; (trace 3) 20-s flash; (trace 4) 30-s flash; (trace 5) 90-s flash. (Insert) Structure of azido-PP$_i$. (B) Fast atom bombardment mass spectrum of purified azido-PP$_i$, showing the corresponding ion at m/z 339.

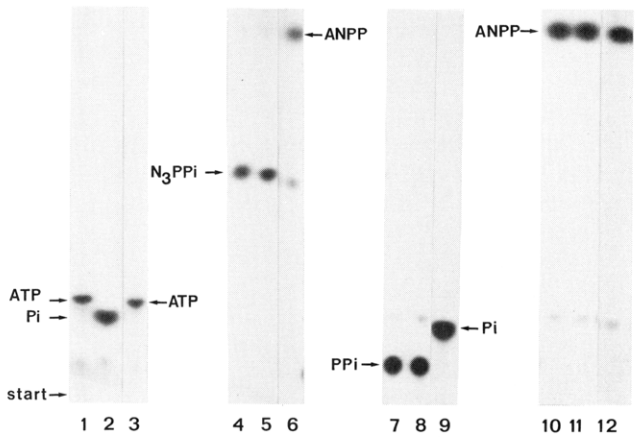

FIGURE 3: Substrate hydrolysis by the mitochondrial F_1-ATPase and yeast inorganic pyrophosphatase (PPase) and analysis of products by chromatography on silica gel plate. [γ-^{32}P]ATP (lane 1) control; (lane 2) incubation with ATPase; (lane 3) incubation with PPase. [α-^{32}P]Azido-PP$_i$ (lane 4) control; (lane 5) incubation with ATPase; (lane 6) incubation with PPase. [^{32}P]PP$_i$ (lane 7) control; (lane 8) incubation with ATPase; (lane 9) incubation with PPase. [^{32}P]ANPP (lane 10) control; (lane 11) incubation with ATPase; (lane 12) incubation with PPase. Experimental conditions are described under Materials and Methods.

remained unchanged. This latter feature differentiates azido-PP$_i$ from ANPP (Lauquin et al., 1980).

The fast atom bombardment mass spectrum of azido-PP$_i$ exhibited three readily attributable pairs of peaks (Figure 2B). The first set of peaks at m/z 339 and 311 corresponded to the parent anion azido-PP$_i$ accompanied by its derivative deprived of N_2. The second set at m/z 177 and 159 was attributed to the PP$_i$ anion and its dehydrated derivative. Likewise, the third set at m/z 97 and 79 was ascribed to the P$_i$ anion and its dehydrated derivative. The m/z 323 signal resulted from the loss of one oxygen on the nitro moiety, while the m/z 46 signal was associated with the nitro anion fragment. The m/z 91 signal was due to fragmentation of the glycerol matrix.

Azido-PP$_i$ Is Hydrolyzed by Inorganic Pyrophosphatase, but Not by F_1-ATPase. Potential substrates assayed with inorganic pyrophosphatase and F_1-ATPase were [α-^{32}P]azido-PP$_i$, [^{32}P]ANPP, [^{32}P]PP$_i$, and [γ-^{32}P]ATP. As shown in Figure 3, only [γ-^{32}P]ATP was hydrolyzed by F_1-ATPase, giving [^{32}P]P$_i$ and ADP (lane 2). As expected, neither [^{32}P]ANPP (lane 11) nor [^{32}P]PP$_i$ (lane 8) was a substrate for this enzyme, corroborating data from Lauquin et al. (1980) and Issartel et al. (1987), respectively. [α-^{32}P]Azido-PP$_i$ was also not hydrolyzed by F_1-ATPase (lane 5). Even after a 45-min incubation at 30 °C of 0.4 mM [α-^{32}P]azido-PP$_i$ with 2 μM F_1 and 3 mM $MgCl_2$, no difference could be detected on the autoradiography of the chromatoplate with respect to a control performed in the absence of F_1. The absence of hydrolysis of azido-PP$_i$ by F_1 was confirmed by using the method of Fiske and Subbarow (1925) to detect P$_i$.

With yeast inorganic pyrophosphatase, [^{32}P]ANPP was not hydrolyzed to any detectable extent after 3 h at 30 °C (lane 12), whereas hydrolysis of [^{32}P]PP$_i$ (lane 9) and [α-^{32}P]azido-PP$_i$ (lane 6) was complete, yielding [^{32}P]P$_i$ and [^{32}P]ANPP, respectively. Taken together, these results indicate that azido-PP$_i$ behaves as an analogue of PP$_i$ toward both F_1 and inorganic pyrophosphatase.

[α-^{32}P]Azido-PP$_i$ Binds to Three Sites on Mitochondrial F_1. The binding of [α-^{32}P]azido-PP$_i$ to F_1 was assayed under the conditions described under Materials and Methods.

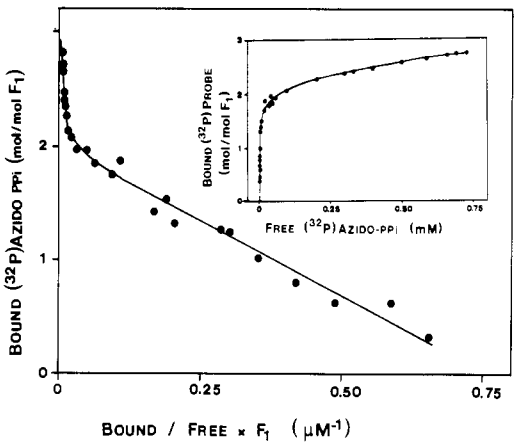

FIGURE 4: Scatchard plot analysis of the azido-PP_i binding sites of mitochondrial F_1 in the absence of photoirradiation. F_1 was incubated in the dark for 30 min at 30 °C with increasing concentrations of [α-^{32}P]azido-PP_i up to 750 μM in medium A (cf. Materials and Methods). F_1-bound radioactivity recovered by centrifugation–filtration was determined by liquid scintillation counting. (Insert) Direct saturation plots.

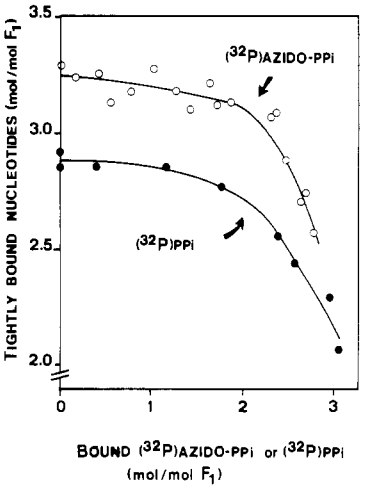

FIGURE 5: Correlation between the reversible binding of [α-^{32}P]-azido-PP_i to mitochondrial F_1 and the decrease in tightly bound nucleotides and comparison with the effect of [^{32}P]PP_i. The amount of bound [α-^{32}P]azido-PP_i and [^{32}P]PP_i was determined by centrifugation–filtration as in Figure 4. The nucleotide content of F_1 was determined as described under Materials and Methods.

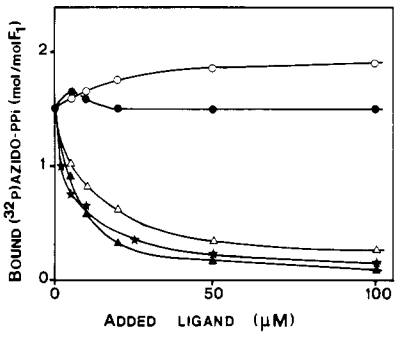

FIGURE 6: Effect of various ligands on the reversible binding of [α-^{32}P]azido-PP_i to F_1. Different phosphate species were incubated at the indicated concentrations with F_1 in the presence of 20 μM [α-^{32}P]azido-PP_i. Conditions were similar to those of the experiment illustrated in Figure 4. (○) P_i; (●) ANPP; (△) PP_i; (☆) AMP-PNP; (▲) ADP.

Equilibrium was reached after 10 min of incubation in the absence of light and was stable for more than 60 min. Similar equilibrium conditions have been reported for PP_i and F_1 (Issartel et al., 1987). In all the experiments described below, a 30-min incubation period was chosen, and this time was also used for P_i and ADP binding.

Native mitochondrial F_1 (cf. Materials and Methods) possesses three tightly bound nucleotides. Titrations carried out with increasing concentrations of [α-^{32}P]azido-PP_i (up to 750 μM) indicate the presence of three binding sites at the plateau of saturation (see Figure 4, insert). The Scatchard plots of the binding data illustrated in Figure 4 can be interpreted on the basis of two independent types of binding sites consisting of two high-affinity sites with a K_d of 2 μM and one low-affinity site with a K_d of about 300 μM. In similar titration experiments conducted with nucleotide-depleted F_1, a plateau of three binding sites at saturation was also found (data not shown).

In agreement with the results obtained with PP_i (Issartel et al., 1987), Mg^{2+} was required for the binding of azido-PP_i. When $MgCl_2$ was replaced by 2 mM EDTA, the amount of bound azido-PP_i was only 0.4 mol/mol of F_1 for a concentration of [α-^{32}P]azido-PP_i of 400 μM, i.e., a nearly saturating concentration in the Mg^{2+} medium.

Saturation Binding of [α-^{32}P]Azido-PP_i to F_1 Induces the Release of One Tightly Bound Nucleotide. [α-^{32}P]Azido-PP_i was added at increasing concentrations to F_1, and for each addition the amount of bound [α-^{32}P]azido-PP_i was determined together with the content of tightly bound nucleotides (cf. Materials and Methods). Filling the two high-affinity azido-PP_i binding sites of F_1 with [α-^{32}P]azido-PP_i had little effect on the amount of tightly bound nucleotides. On the contrary, the binding of the third [α-^{32}P]azido-PP_i to the low-affinity site was correlated with the release of nearly one tightly bound nucleotide (Figure 5). This effect parallels that demonstrated by Issartel et al. (1987) for pyrophosphate.

Diphosphate and Triphosphate Species Compete with Binding of [α-^{32}P]Azido-PP_i on F_1, whereas Monophosphate Species Do Not. The competitive effect of P_i and several phosphate derivatives on the binding of [α-^{32}P]azido-PP_i to F_1 was investigated by using a concentration of photoprobe of 20 μM, leading to the filling of 1.5 sites of the two high-affinity sites of F_1. As illustrated in Figure 6, the ligands used fell into two classes, depending on their competitive efficiency. Competing ligands were ADP, AMP-PNP, and PP_i in order of decreasing efficiency of competition. On the other hand, ANPP and P_i exhibited no such an effect, and P_i even stimulated [α-^{32}P]azido-PP_i binding. In this respect, azido-PP_i behaves as a polyphosphate analogue.

Low Concentrations of Azido-PP_i Stimulate [^{32}P]P_i Binding to F_1. The amount of [^{32}P]P_i bound to F_1 in the presence of increasing concentrations of azido-PP_i was assayed at 50 μM [^{32}P]P_i and 2 μM F_1 in medium A, where the enhancing effect of PP_i was the more drastic (Issartel et al., 1987). In the absence of any stimulating species, bound [^{32}P]P_i amounted to 0.18 mol/mol of F_1 (Figure 7). When the azido-PP_i concentration was increased, the amount of bound [^{32}P]P_i was enhanced to reach a maximum of 0.5 mol of [^{32}P]P_i bound/mol of F_1, coinciding with an azido-PP_i concentration of 10 μM. This was followed by a slow decrease of [^{32}P]P_i binding down to the initial value. Comparison with the PP_i control curve highlights the similarity of effect of PP_i and azido-PP_i on P_i binding and their difference from ADP, which is a marked inhibitor of P_i binding. It is noteworthy that the maximum stimulatory effect was obtained with less azido-PP_i (10 μM) than PP_i (40 μM), although stimulation was of similar magnitude in both cases. Taking the differences in affinity of these ligands into account, the above concentrations correspond to a molar binding stoichiometry of about 1.5 in both cases.

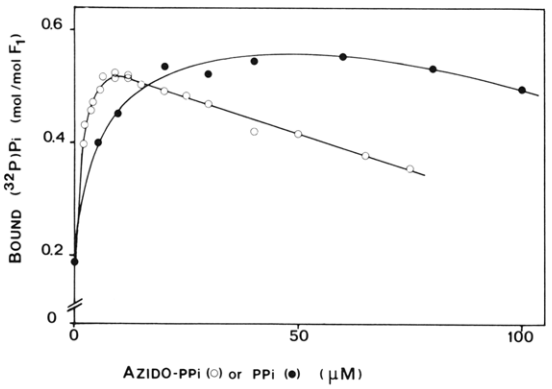

FIGURE 7: Compared effect of low concentrations of (○) azido-PP_i and (●) PP_i on the reversible binding of [^{32}P]P_i by mitochondrial F_1-ATPase. Conditions were similar to those described in the legend to Figure 4. [^{32}P]P_i was used at the concentration of 50 μM in the presence of increasing concentrations of unlabeled azido-PP_i or PP_i.

Sulfite Is a Weak Competitor for both ADP and Azido-PP_i. Anions of the Hofmeister series have been explored by Ebel and Lardy (1975) for their stimulatory effects on mitochondrial F_1-ATPase. It was recently reported that PP_i behaves like the oxyanion sulfite on the kinetics of ATP hydrolysis by mitochondrial F_1-ATPase by preventing the decrease in ATPase activity which develops during ATP hydrolysis, and it was concluded that PP_i does not interact with the catalytic sites of F_1 (Kalashnikova et al., 1988). In contrast, our previous results (Issartel et al., 1987) favored the hypothesis that PP_i was recognized by the catalytic sites of F_1. To clarify this point, experiments were devised for a better definition of the interactions between the binding sites for ADP, PP_i, and anions. A number of anions were found to compete with [α-^{32}P]azido-PP_i for binding to F_1. Sulfite proved to be the most efficient anion among those assayed. In the order of efficiency, they were sulfite = thiosulfate > 2,4-dinitrophenol = sulfate > carbonate > nitrate > disulfite. Borate, azide, and arsenate were without effect, whereas P_i had a marked stimulatory effect. The inhibitory effect of 5 mM sulfite was also investigated on the binding of both [α-^{32}P]azido-PP_i and [^{3}H]ADP, the two ligands being used at concentrations ranging between 0 and 10 μM and between 0 and 3 μM, respectively. Incubation and treatment were as described under Materials and Methods, the presence of 50 mM NaCl in the medium favoring the specific effect of sulfite. Under these conditions, the maximal binding stoichiometry for both [α-^{32}P]azido-PP_i and [^{3}H]ADP was 2 mol of ligand/mol of F_1. With respect to binding affinity, the two liganded sites were homogeneous, with K_d = 2 μM for azido-PP_i and K_d = 0.3 μM for ADP. Sulfite competed for the binding of both [α-^{32}P]azido-PP_i and [^{3}H]ADP with K_i values of 1.2 and 2.5 mM, respectively (data not illustrated). These results provide evidence that ADP and PP_i bind to a closely related site in F_1 since the binding of both ligands was similarly affected by sulfite. The simplest way to rationalize this observation, in the absence of direct demonstration of a presumed anion-binding site by direct binding assay, is to consider that sulfite acts either by binding at the level of the catalytic site of F_1 or by affecting the overall conformation of the enzyme.

Photoinactivation and Photolabeling of F_1-ATPase by [α-^{32}P]Azido-PP_i. Preincubation of F_1 with [α-^{32}P]azido-PP_i in the dark for 30 min at 30 °C followed by photoirradiation for a brief period of time (4 × 30 s) resulted in inactivation of F_1-ATPase and the concomitant covalent incorporation of radioactivity into F_1 (Figure 8). There was no significant loss of activity in the absence of probe. The extent of photolabeling

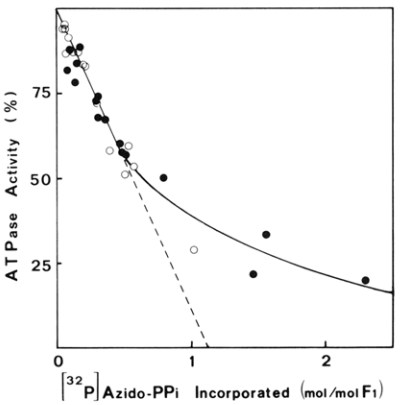

FIGURE 8: Correlation between covalent binding of [α-^{32}P]azido-PP_i upon photoirradiation and photoinactivation of F_1-ATPase. Incubation was conducted in the presence of increasing concentrations of [α-^{32}P]azido-PP_i up to 500 μM in medium A for 30 min at 30 °C in the dark. The samples were then subjected to four successive photoirradiations of 30 s. After photoirradiation, samples were treated as discussed under Materials and Methods and assayed for ATPase activity, bound radioactivity, and protein content. (○) Heat denaturation; (●) acid denaturation.

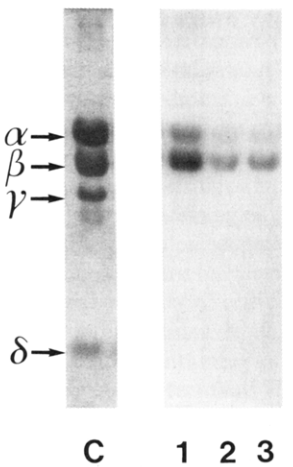

FIGURE 9: Photolabeling of the mitochondrial F_1-ATPase with [α-^{32}P]azido-PP_i. F_1 was labeled with 30 μM [α-^{32}P]azido-PP_i with or without protection by specific ligands. The labeled subunits were analyzed by TDAB–polyacrylamide gel electrophoresis followed by autoradiography. (Lane C) Coomassie blue staining. (Lanes 1–3) Autoradiography: (lane 1) F_1 control; (lane 2) protection by ADP (5 mM); (lane 3) protection by PP_i (5 mM).

was varied by increasing the concentration of [α-^{32}P]azido-PP_i from 2 to 500 μM. Up to 50% inactivation, the plots were rectilinear. Above 50% inactivation, they became curvilinear. As drastic denaturation procedures were used before the bound radioactivity was counted, retention of noncovalently bound probe is unlikely. By extrapolation of the rectilinear plots obtained below 50% inactivation, it was found that 100% inactivation corresponded to 1.1 mol of azido derivative bound/mol of F_1.

Aliquots recovered after centrifugation–filtration on Sephadex G-50 were subjected to a TDAB–polyacrylamide gel electrophoresis. The totality of the radioactivity was associated with the major subunits α and β, most of it being located on β (Figure 9, lanes C and 1). As expected, PP_i as well as ADP exerted a marked protective effect on the photolabeling (about 80%) (Figure 9, lanes 2 and 3, respectively).

Discussion

A new photoaffinity probe, 4-azido-2-nitrophenyl pyrophosphate (azido-PP_i), has been synthesized in its radioactive form with ^{32}P placed in the α position. It adds to a list of

photoprobes that have been used in structural and functional studies of the catalytic site of F_1 (Lunardi & Vignais, 1985).

Azido-PP_i as a Polyphosphate Analogue. ANPP, the precursor of azido-PP_i, is a phosphate analogue (Lauquin et al., 1980) that has been used to map the P_i binding site of F_1 (Garin et al., 1989). Azido-PP_i was therefore expected to behave as a diphosphate analogue. Indeed, the following lines of evidence point to the analogy of azido-PP_i with polyphosphate ligands. (1) Azido-PP_i binds to three sites on mitochondrial F_1 with K_d values of 2 and 300 μM, comparable to the K_d values of 1 and 20 μM obtained for PP_i binding (Issartel et al., 1987). A total of three binding sites for azido-PP_i and PP_i are also encountered on the nucleotide-depleted enzyme. (2) PP_i, ADP, and the ATP analogue AMP-PNP compete efficiently with azido-PP_i for binding to F_1. This is not the case for the monophosphate species, i.e., P_i, and its analogue, ANPP. (3) Azido-PP_i is recognized and cleaved by the yeast inorganic pyrophosphatase, but not by mitochondrial F_1. (4) The most efficient protection against photolabeling of F_1 by azido-PP_i is obtained with ADP and PP_i. These results taken together suggest that azido-PP_i behaves as a diphosphate analogue.

Azido-PP_i as an Analogue of PP_i. Although PP_i has a number of features in common with ADP, it exhibits peculiar features of its own [cf. Kironde and Cross (1986), Issartel et al. (1987), and Kalashnikova et al. (1988)]. As far as its effects on mitochondrial F_1 are concerned, azido-PP_i shares some properties with PP_i. (1) The filling of three sites of F_1 by azido-PP_i or PP_i is correlated with the release of one tightly bound nucleotide from a nonreadily exchangeable site. (2) Low concentrations of azido-PP_i or PP_i stimulate the binding of P_i to a high-affinity P_i binding site, and the maximal extent of stimulation of P_i binding is the same with the two ligands. On the other hand, the yeast inorganic pyrophosphatase hydrolyzes PP_i rapidly, but is without effect on ADP. The fact that azido-PP_i is bound and hydrolyzed by this enzyme strongly favors the contention that it is an analogue of PP_i.

What Is the Nature of the Sites of F_1 Recognized by Azido-PP_i? Given the complexity of ligand binding to F_1, it is worthwhile to discuss the nature of the PP_i binding sites. As stated by Kironde and Cross (1986), the three nucleotides tightly bound to desalted F_1 are located in one catalytic and two noncatalytic sites. As a consequence, desalted F_1 exhibits one noncatalytic site and two catalytic sites free of nucleotides. Our enzyme prepared, stored, and desalted under the same conditions as those described by Kironde and Cross (1986) (see Materials and Methods) is presumed to bind substrates to these three vacant sites.

A number of observations strengthen the idea that PP_i is recognized only at the level of the catalytic sites: (1) The vacant noncatalytic site in native and desalted F_1 is highly specific for adenine nucleotides, and conversely IDP, GDP, CDP, and PP_i do not affect the retention of adenine nucleotide on the noncatalytic site (Kironde & Cross, 1986). (2) The binding of three PP_i or three azido-PP_i per native and desalted F_1 promotes the dissociation of only one nucleotide. This finding can be simply explained by direct competition between PP_i and the nucleotide already bound to the tight catalytic site. (3) When F_1 depleted of the tightly bound nucleotides is used, the total number of sites for PP_i or azido-PP_i never exceeds three, indicating that these ligands are unable to interact with the nonexchangeable noncatalytic binding sites. (4) Of the three binding sites for azido-PP_i in native and desalted F_1, two exhibit the same high affinity. Consequently, they must be photolabeled indistinctly, and their photolabeling is expected to result in the same yield of photoinactivation. This is indeed consistent with the fact that, by extrapolating binding data to zero activity, complete inactivation of F_1 is found to require 1 mol of [^{32}P]azido-PP_i bound/mol of F_1 (Figure 8). In brief, it is unlikely that azido-PP_i binds to a noncatalytic site and a catalytic one. Furthermore, the partial site reactivity exhibited by F_1 and reflected by full inactivation of F_1 upon photolabeling by one azido-PP_i is explained by a cooperative mechanism between alternating catalytic sites as discussed in the case of other photoprobes (Vignais & Lunardi, 1985; Boulay et al., 1985; Garin et al., 1989).

It is interesting that P_i does not compete with azido-PP_i for binding to F_1; this could be explained by assuming that P_i binds to the same site as the γ phosphate group of ATP as recently discussed by Garin et al. (1989), while the binding subsite for PP_i would coincide with the region recognized by the $\alpha\beta$ phosphate groups of ADP or ATP in the nucleotide-binding site. As illustrated in Figure 9, azido-PP_i binds covalently not only at the level of the β subunit, which is the catalytic subunit, but also on the α subunit, although labeling of the α subunit is substantially lower than that of the β subunit. It must be kept in mind that the azidonitrophenol moiety of azido-PP_i has a nonnegligible size. Consequently, whereas azido-PP_i is expected to photolabel predominantly the β subunit in the region of the catalytic site, it might also photolabel amino acids located in a juxtaposed α subunit at short distance from the catalytic site.

Anions such as sulfite have been shown to have some properties analogous to those of PP_i. However, in contrast to PP_i and azido-PP_i, their effects are developed only in the millimolar range as evidenced by the K_i values for the competitive effect on the binding of both ADP and azido-PP_i. An apparent competitive interaction between ADP and sulfite for stimulation of chloroplast F_1 has also been reported (Larson & Jagendorf, 1989), and it was hypothesized that sulfite, when placed at the end of ADP, results in a composite structure that might simulate ATP chemically. In this context, it may be suggested that sulfite either binds with low affinity to the same site as ADP and PP_i or affects the overall conformation of F_1, so that the affinity of F_1 for these ligands is lowered. To date, we have no argument to favor either of these hypotheses.

ACKNOWLEDGMENTS

We thank J. Bournet for typing the manuscript.

Registry No. F_1, 9000-83-3; PP_i, 14000-31-8; ADP, 58-64-0; AMP-PNP, 25612-73-1; azido-PP_i, 123883-88-5; [α-^{32}P]azido-PP_i, 123883-89-6; [^{32}P]ANPP, 123883-90-9; sulfite, 14265-45-3; inorganic pyrophosphatase, 9033-44-7.

REFERENCES

Boulay, F., Dalbon, P., & Vignais, P. V. (1985) *Biochemistry 24*, 7372–7379.

Bradford, M. M. (1976) *Anal. Biochem. 72*, 248–254.

Bronnikov, G. E., & Zakharov, S. D. (1983) *Anal. Biochem. 131*, 69–74.

Ebel, R. E., & Lardy, H. A. (1975) *J. Biol. Chem. 250*, 191–196.

Fiske, C. H., & Subbarow, Y. (1925) *J. Biol. Chem. 66*, 375–400.

Garin, J., Michel, L., Dupuis, A., Issartel, J.-P., Lunardi, J., Hoppe, J., & Vignais, P. V. (1989) *Biochemistry 28*, 1442–1448.

Garrett, N. E., & Penefsky, H. S. (1975) *J. Biol. Chem. 250*, 6640–6647.

Hoard, D. E., & Ott, D. C. (1965) *J. Am. Chem. Soc. 87*, 1785–1788.

Issartel, J.-P., Lunardi, J., & Vignais, P. V. (1986) *J. Biol. Chem. 261*, 895–901.
Issartel, J.-P., Favre-Bulle, O., Lunardi, J., & Vignais, P. V. (1987) *J. Biol. Chem. 262*, 13538–13544.
Kalashnikova, T. Y., Milgrom, Y. M., & Murataliev, M. B. (1988) *Eur. J. Biochem. 177*, 213–218.
Kironde, F. A. S., & Cross, R. L. (1986) *J. Biol. Chem. 261*, 12544–12549.
Klein, G., Satre, M., Zaccaï, G., & Vignais, P. V. (1982) *Biochim. Biophys. Acta 681*, 226–232.
Knowles, A. F., & Penefsky, H. S. (1972) *J. Biol. Chem. 247*, 6617–6623.
Larson, E. M., & Jagendorf, A. T. (1989) *Biochim. Biophys. Acta 973*, 67–77.
Lauquin, G., Pougeois, R., & Vignais, P. V. (1980) *Biochemistry 19*, 4620–4626.
Lundin, A., Rickardson, A., & Thore, A. (1976) *Anal. Biochem. 75*, 611–620.
Penefsky, H. S. (1977) *J. Biol. Chem. 252*, 2891–2899.
Penin, F., Godinot, C., & Gautheron, D. C. (1984) *Biochim. Biophys. Acta 775*, 239–245.
Senior, A. E. (1988) *Physiol. Rev. 68*, 177–231.
Vignais, P. V., & Lunardi, J. (1985) *Annu. Rev. Biochem. 54*, 977–1014.
Walker, J. E., Fearnley, I. M., Gay, N. J., Gibson, B. W., Northrop, F. D., Powell, S. J., Runswick, M. J., Saraste, M., & Tybulewicz, V. L. J. (1985) *J. Mol. Biol. 184*, 677–701.

Substitution of Amino Acids in Helix F of Bacteriorhodopsin: Effects on the Photochemical Cycle†

Patrick L. Ahl,‡,§ Lawrence J. Stern,∥,⊥ Tatsushi Mogi,∥,# H. Gobind Khorana,∥ and Kenneth J. Rothschild*,‡

Departments of Physics and Physiology, Boston University, 590 Commonwealth Avenue, Boston, Massachusetts 02215, and Departments of Biology and Chemistry, Massachusetts Institute of Technology, Cambridge, Massachusetts 02139

Received April 18, 1989; Revised Manuscript Received July 21, 1989

ABSTRACT: The effects of amino acid substitutions in helix F of bacteriorhodopsin on the photocycle of this light-driven proton pump were studied. The photocycles of Ser-183→Ala and Glu-194→Gln mutants were qualitatively similar to that of wild-type bacteriorhodopsin produced in *Escherichia coli* and bacteriorhodopsin from *Halobacterium halobium*. The substitution of a Phe for either Trp-182 or Trp-189 significantly reduced the fraction of photocycling bacteriorhodopsin. The amino acid substitutions Tyr-185→Phe and Ser-193→Ala substantially increased the lifetime of the photocycle without substantially increasing the lifetime of the M photocycle intermediate. Similar results were also obtained with the Pro-186→Gly substitution. In contrast, replacing Pro-186 with the larger residue Leu inhibited the formation of the M photocycle intermediate. These results are consistent with a structural model of the retinal-binding pocket suggested by low-temperature UV/visible and Fourier transform infrared difference spectroscopies that has Trp-182, Tyr-185, Pro-186, and Trp-189 forming part of the binding pocket.

Bacteriorhodopsin (bR)[1] is a light-driven proton pump in the purple membrane of *Halobacterium halobium*. The amino acid sequence contains seven hydrophobic regions labeled A–G that correspond to the seven transmembrane helices[2] (Henderson & Unwin, 1975; Khorana et al., 1979; Ovchinnikov et al., 1979; Huang et al., 1982). The chromophore, *all-trans*-retinal, is covalently linked to Lys-216 in helix G through a protonated Schiff base (Bayley et al., 1981; Katre et al., 1981; Rothschild et al., 1982). Light absorption by retinal initiates the bR photocycle by causing isomerization about the 13–14 double bond (Braiman & Mathies, 1982). The photocycle, which occurs on a millisecond time scale at room temperature, involves at least five intermediates:[3] $BR_{568} \rightarrow K_{610} \rightarrow L_{550} \rightarrow M_{412} \rightarrow O_{640} \rightarrow BR_{568}$ (Lozier et al., 1975). There is also considerable evidence for a sixth intermediate, N, between M and O which has a λ_{max} near 550 nm (Dancsházy et al., 1988; Kouyama et al., 1988; Nagle et al., 1982; Xie et al., 1987).

Site-directed mutagenesis can be used to examine the role of individual amino acids in the structure and function of

† Supported by grants from the National Science Foundation (DMB-8806007) and the Office of Naval Research (N00014-88-04164) to K.J.R.; grants from the National Science Foundation (PCM-8110992), National Institutes of Health (GM28289-06 and AI-11479), and Office of Naval Research, Department of the Navy (N00014-82-K-0668) to H.G.K.; and a postdoctoral fellowship from American Heart Association Massachusetts Affiliate to P.L.A. L.J.S. is a NIH predoctoral trainee.

* To whom correspondence should be addressed at the Department of Physics, Boston University, 590 Commonwealth Ave., Boston, MA 02215.
‡ Boston University.
§ Present address: Department of Pathology and Laboratory Medicine, Hahnemann University, Philadelphia, PA 19102.
∥ Massachusetts Institute of Technology.
⊥ Present address: Departments of Biochemistry and Molecular Biology, Harvard University, Cambridge, MA 02138.
Present address: Department of Biology, Faculty of Science, University of Tokyo, Hongo, Tokyo 113, Japan.

[1] Abbreviations: AU, absorbance unit; bR, bacteriorhodopsin; FTIR, Fourier transform infrared; ebR, bacteriorhodopsin produced in *E. coli*; PM, purple membrane; W182F, Trp-182→Phe; S183A, Ser-183→Ala; Y185F, Tyr-185→Phe; P186G, Pro-186→Gly; P186L, Pro-186→Leu; W189F, Trp-189→Phe; S193A, Ser-193→Ala; E194Q, Glu-194→Gln.

[2] Amino acids in the putative bR helices A–G are based on the folding model proposed by Huang et al. (1982).

[3] BR designates the light-adapted state of bacteriorhodopsin. The subscripts indicate the λ_{max} of the photocycle intermediates. The wavelength subscript designations for BR and the photocycle intermediates are not used throughout the rest of this paper since the λ_{max} values vary for many of the mutants [see Ahl et al. (1988)].

0006-2960/89/0428-10028$01.50/0